Comparative Biochemistry and Physiology, Part C 190 (2016) 48–53

Contents lists available at ScienceDirect

Comparative Biochemistry and Physiology, Part C

journal homepage: www.elsevier.com/locate/cbpc

Morphological and functional alteration of erythrocyte ghosts and giant unilamellar vesicles caused by *Vipera latifi* venom

Gayane Kirakosyan, Maryam Mohamadvarzi, Lusine Ghulikyan, Naira Zaqaryan, Arsen Kishmiryan, Naira Ayvazyan *

Orbeli Institute of Physiology, National Academy of Sciences of the Republic of Armenia, Orbely str. 22, 0019 Yerevan, Armenia

ARTICLE INFO

Article history:
Received 19 May 2016
Received in revised form 10 August 2016
Accepted 16 August 2016
Available online 21 August 2016

Keywords:
Vipera latifi
Erythrocyte ghosts
GUVs
$[Na^+,K^+]$-ATPase and $(Ca^{2+} + Mg^{2+})$-ATPases

ABSTRACT

Snake bites are an endemic public health problem in Iran, both in rural and urban area. Viper venom as a hemolytic biochemical "cocktail" of toxins, primarily cause to the systemic alteration of blood cells. In the sixties and seventies, human erythrocytes were extensively studied, but the mechanical and chemical stresses commonly exerted on red blood cells continue to attract interest of scientists for the study of membrane structure and function. Here, we monitor the effect of *Vipera latifi* venom on human erythrocytes ghost membranes using phase contrast and fluorescent microscopy and changes in ATPase activity under snake venom influence *in vitro*. The ion pumps $[Na^+,K^+]$-ATPase and $(Ca^{2+} + Mg^{2+})$-ATPase plays a pivotal role in the active transport of certain cations and maintenance of intracellular electrolyte homeostasis. We also describe the interaction of *Vipera latifi* (VL) venom with giant unilamellar vesicles (GUVs) composed of the native phospholipid mixtures visualized by the membrane fluorescence probe, ANS, used to assess the state of membrane and specifically mark the phospholipid domains.

1. Introduction

Iranian herpetofauna is very rich by venomous snakes, including the representatives of the all three most important groups causing envenomation: Elapidae, Crotalidae and Viperidae. There are 83 snake species in Iran and about 25 of them are venomous (Latifi, 1991; Kakanj et al., 2015). Due to medical statistics there were about 53,787 snake envenomations that caused 67 mortalities in Iran within 2002–2011 (Dehghani et al., 2014). *Vipera latifi* (also denominated *Montivipera latifi* by some authors (Wallach et al., 2014)) belongs to sister clades of the Middle East complex within the monophyletic Eurasian Vipera genus (Nilson et al., 1999; Lenk et al., 2001). These snakes are important culprits of snake bite in Iran each year, leading to severe local effects, such as tissue blistering, hemorrhage and necrosis, as well as coagulopathy, especially clotting disorders and hypofibrinogenemia (Dehghani et al., 2014; Latifi, 1984; Kakanj et al., 2015). Venom yield per snake is around 6 ± 2 mg and the LD50 (median lethal dose) values for mouse are 3.2–7.9 μg/mouse (Latifi, 1984, 1991). Although the venoms of *Vipera latifi* haven't been yet thoroughly characterized at proteomic level (Latifi et al., 1965), their toxinological profile is quite well studied (Dehghani et al., 2014; Latifi, 1984), but the information about the correlation with the clinical picture of envenoming still lacks.

Studies on hemolytic action of snake venoms on human red blood cells (RBCs) have been carried out since the 1960s (Ibrahim and Thompson, 1965). Recent advances in fluorescent and super-resolution microscopy cause the new wave of re-investigations of cell-invasive mechanisms of snake venoms (Flachsenberger et al., 1995). After extrusion of nuclei and degradation of endoplasmic reticulum, reticulocytes emerge in the circulation; here they rapidly develop into mature RBCs 8 μm biconcave disks and with 120 days life span (Yau et al., 2012). The flexibility of the membrane along with the ability of RBCs to maintain their morphology without a nucleus makes them an excellent model to study membrane mechanics. Healthy RBCs have a characteristic shape and yet they can alter their morphology to become either spherocytes (spherical shape), various forms of echinocyte (a spherical shape with rounded spiky protrusions) or stomatocytes (swollen cup-shaped cells) (Babu, 2009). These shape changes can be imposed either by outside hydrodynamic forces in the vascular system, in response to ATP depletion, chemical mediators (amphipathic molecules) or a physical environment like the surface of glass (Elgsaeter et al., 1986; Elgsaeter and Mikkelsen, 1991).

The human RBC membrane content is similar with most of animal membranes and it is composed by: 19.5% (w/w) of water, 39.5% of proteins, 35.1% of lipids and 5.8% of carbohydrates (Oliveira and Saldanha, 2010; Pasini et al., 2006).

In present stage of investigations we'd like to try going further in modeling of viper venom interaction with biological membranes and its possible traumatic or therapeutic effect (Ghazaryan et al., 2015a; 2015b). We propose to characterize the morphological changes of RBC membranes opposite to giant unilamellar vesicles, as a so called negative control, because they have a lipid membrane free of proteins. Also we propose to assess the alteration of the normal work of main ion

* Corresponding author at: Lab of Toxinology, Orbeli Institute of Physiology, National Academy of Sciences of the Republic of Armenia, Orbely str. 22, 0019 Yerevan, Armenia.
E-mail address: taipan@ysu.am (N. Ayvazyan).

http://dx.doi.org/10.1016/j.cbpc.2016.08.006
1532-0456/

transporters of RBC membrane in course of treatment with *Vipera latifi* venom. Changes both in lipid composition and protein condition modulate membrane transport processes. Red blood cells (RBC) from patients with various types of pathology show significant membrane abnormalities (Klop et al., 2013), and it has been suggested that disorder of some important cell pumps play a role in producing and further spreading of these abnormalities. Sodium pump Na^+,K^+-ATPase plays an essential role in cellular function and is altered in a variety of pathological conditions (Coka-Guevara et al., 1999; Kassák et al., 2006). Theoretically, the increasing of intracellular Na^+ would lead to decrease the inward Na^+ gradient, which may drive Ca^{2+} efflux through Ca^{2+}-Na^+ counter transport. The human RBC contains an outwardly directed Ca^{2+} pump, the activity of which is coupled to phosphorylation and hydrolysis of a 150 kDa membrane-bound, Ca^{2+}-activated, Mg^{2+}-dependent ATPase (Vincenzi et al., 1986). In the present study erythrocyte ghost membranes Na^+,K^+-ATPase and Ca^{2+}-activated Mg^{2+}-dependent ATPase activities have been analyzed in course of envenomation by the *Vipera latifi* venom.

2. Materials and methods

2.1. Reagents and venom

VL venom was purchased from Latoxan. ANS (8-anilino-1-naphthalene sulfonic acid) and ouabain was purchased from Sigma. Packed red blood cells (PRBCs) were obtained from Haemathology Center after Prof. R. Yeolyan (Ministry of Health, Republic of Armenia).

2.2. Phospholipid processing

The phospholipid fraction was separated from the bovine brain according to the Muller method (Mueller et al., 1962). White matter was dissected from fresh adult bovine brain and scraped free of gray matter. The white matter was homogenized with 1:1 chloroform–methanol mixture (1 g of tissue/20 mL). The suspension was washed with distilled water to remove non-lipid substances. Then a vacuum pump was used to remove the chloroform–methanol mixture. The remaining phospholipid composition was dissolved in the chloroform–methanol solution (1:2), which is stable for months if stored in the dark at 0 till −15 °C temperature, preferably, with no air space.

2.3. Giant unilamellar vesicles

GUVs were prepared by the electroformation method, developed by Angelova et al. (1992). GUVs were formed in a temperature controlled chamber that allows a working temperature range from 20 °C to 50 °C. GUVs were prepared using the following steps: ~2 μL of the phospholipid stock solution was spread on each of the two sample chamber platinum wires. The chamber was then dried for ~1 h to remove any remaining trace of organic solvent (nonane). The chamber and the buffer (Tris–HCl 0.5 mM, pH 7.4) were separately equilibrated to temperatures above the lipid mixture phase transition(s) (~10 °C over the corresponding transition temperature, which is close to 30 °C) and then 2 mL of buffer was added to cover the wires. Immediately after buffer addition, the platinum wires were connected to a function generator and a low-frequency AC (alternating current) field (sinusoidal wave function with a frequency of 10 Hz and amplitude of 2 V) was applied for 90 min. The mean diameter of these GUVs should be ~30 μm, as previously reported (Sanchez et al., 2001; Ayvazyan and Ghazaryan, 2012).

2.4. Erythrocyte ghosts

Erythrocyte membranes were obtained by the method of Dodge et al. (1956). Protein was measured by the method of Lowry as described (Lowry et al., 1951) using bovine serum albumin as a standard. To obtain erythrocyte ghosts, after the last wash the RBC pellet was mixed with nine volumes of ice-cold lysis buffer (5 mM sodium phosphate) and stirred for 15 min at 0 °C. Subsequently, the unsealed erythrocyte ghosts were pelleted by centrifugation at 37,000 × *g* for 10 min at 0 °C. After the centrifugation the ghosts were washed with ice-cold lysis buffer until residual hemoglobin was not visible. The RBC ghosts were suspended in about 0.5 volume of PBS and were kept frozen at −30 °C until use.

2.5. Fluorescence labeling and microscopy

The membrane fluorescence probe ANS (8-anilino-1-naphthalene sulfonic acid) was used for visualization of GUVs and erythrocyte ghosts. 1 μM ANS added to the sample chamber after the vesicle formation and then incubated for 5 min at 25 °C (Verstraeten et al., 2005). Images were collected on a fluorescence microscope FM320-5M (AmScope, USA). The excitation and emission wavelengths for ANS were 360 nm and 490 nm, respectively (Ayvazyan and Ghazaryan, 2012). Phase-contrast imaging was done on the Nikon microscope with 9MP digital camera (AmScope, USA).

2.6. Na^+/K^+ and Ca^{2+}/Mg^{2+}-ATPase assay in RBC

The activities of the ion motive ATPases, Na-K-ATPase, Ca^{2+}, Mg^{2+}-ATPase, determined by the method of Hesketh et al. (1978). The reaction mixtures for Na^+, K^+-ATPase assay contained 2 mM MgCl2, 150 mM NaCl, 17.5 mM KCl, and 10.0 mM Tris-HCl, pH 7.4, the ghost suspension, in the presence or absence of ouabain (2 mM) (Kassák et al., 2006) and three concentrations of snake venom (pharmacologically relevant to low, sublethal and lethal concentrations according to the LD50 for mouse). Na^+,K^+-ATPase activity was calculated as the difference between the presence or absence of ouabain-sensitive Na^+,K^+-ATPase activity. The reaction mixtures for Ca^{2+}, Mg^{2+} ATPase assay contained 300 μM $CaCl_2$, 2 mM $MgCl_2$, 10.0 mM Tris-HCl, pH 7.4 and the ghost suspension. The values were expressed as the difference between ATPase activity in presence of Mg^{2+}, Ca^{2+} and in presence of Mg^{2+} only. The reaction was initiated by the addition of ATP (7 mM) and mixture was incubated for 1 h at 37 °C. The reaction was stopped by the addition of 10% (wt/vol) ice cold trichloroacetic acid (final conc.). The mixture centrifuged at 4000*g* for 5 min after standing 20 min at 4 °C. The supernatant used for the estimation of inorganic phosphate liberated according to standard method of Fiske and Subbarrow (1925). The activity of each enzyme was expressed as nmol Pi/mg protein/min.

2.7. Statistical analysis

For quantitative analysis of ATPase activity values, results are reported as means ± SEM. The significance of differences between the means was assessed by ANOVA followed by Bonferroni's test when various experimental groups were compared with the control group. A value of $P < 0.05$ indicated significance.

3. Results

3.1. Morphological alterations of ghost membranes

Light microscopy of human erythrocytes revealed a normal ~7.5 μm biconcave disk structure. The venom addition produced marked changes in size and shape of RBC (Fig. 1), these changes included a formation of characteristical rounded spiky protrusions (echinocyte) followed by increasing of RBC size and final lyses (if the concentration of venom is pharmacologically relevant to the sub-lethal and lethal doses). The erythrocyte ghosts are spherical and have a bigger size compare to the normal RBC (Fig. 2A). There was a significant decrease of the ghost diameter after envenoming (Fig. 2B), but interestingly this decrease was reversible and the secondary increasing of erythrocyte

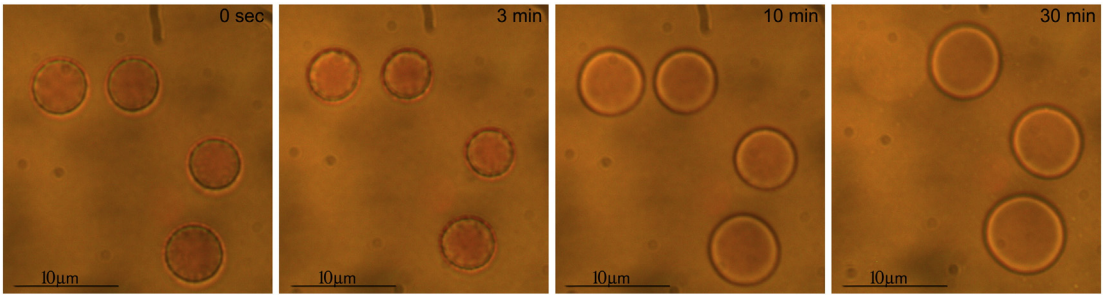

Fig. 1. *Vipera latifi* venom-dependent changes of the intact erythrocytes size and shape is shown. Dried lyophilized toxin of VL was dissolved in Tris-HCl buffer (pH 7.4) with a final concentration of $3 * 10^{-5}$ M, and 1.1 μL of this solution were added to the fluorescent microscope sample.

ghosts' size was observed at all times, when the processing with venom was done with a lower concentration of venom (Fig. 2C). The second addition of the same amount of venom led to the shrinking of the erythrocyte ghosts again, but this time the effect is irreversible (Fig. 2G–I). The first rapid changes of size usually occurred in 1 min, and diameter decreased almost on 50%. The one interesting observation was that erythrocyte ghosts with abnormal primary small size could be shrinking until the complete lyses even after the first addition of the low concentration of venom (Fig. 2A–C, right).

The solubilization process of erythrocyte ghosts by the VL venom was observed also with phase contrast and fluorescence microscopy. A solution of 1.1 μl of venom was injected with a micropipette placed close to the selected ghosts. After contact with the venom solution, all erythrocyte ghosts observed were partially damaged, as detected by a clear decrease in vesicle size. Fig. 3 shows one such example observed under phase contrast microscopy. After only 10 s of venom injection, part of the ghosts is detached and then solubilized in a few seconds (Fig. 3B–C). In this picture it is clear that erythrocyte membrane has

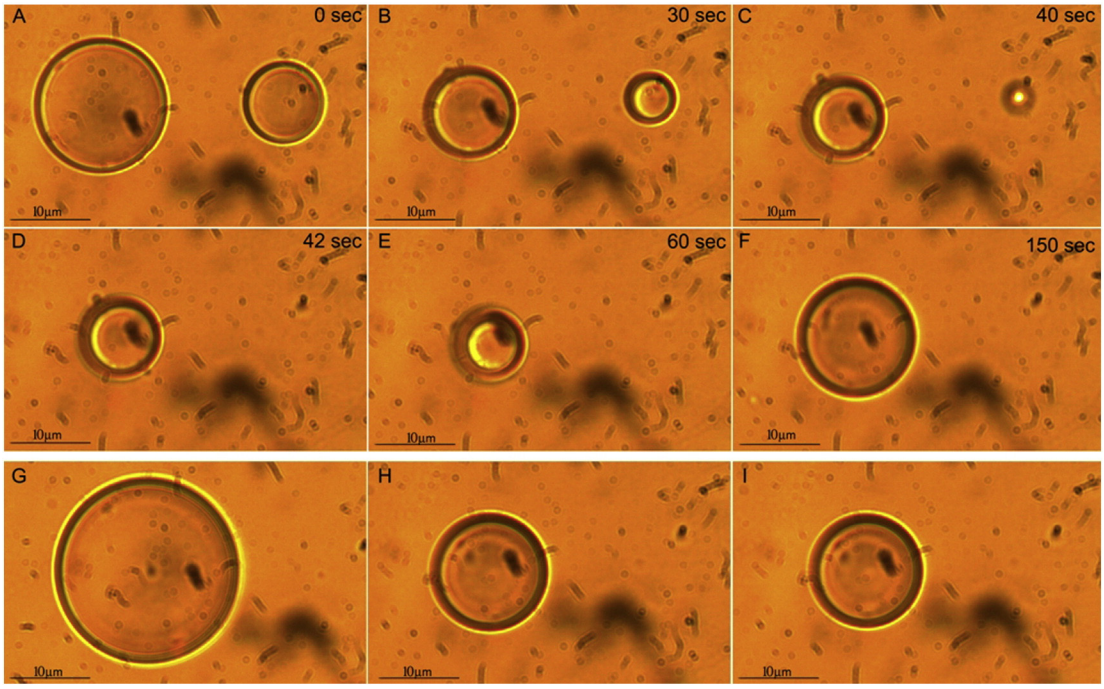

Fig. 2. *Vipera latifi* venom-dependent changes of the erythrocyte ghosts' size is shown. Erythrocyte ghosts were prepared as described in Section 2.4. Dried lyophilized toxin of VL was dissolved in Tris-HCl buffer (pH 7.4) with a final concentration of $3 * 10^{-5}$ M, and 1.1 μL of this solution were added to the microscope sample (A–F), and once again after three minutes (G–I).

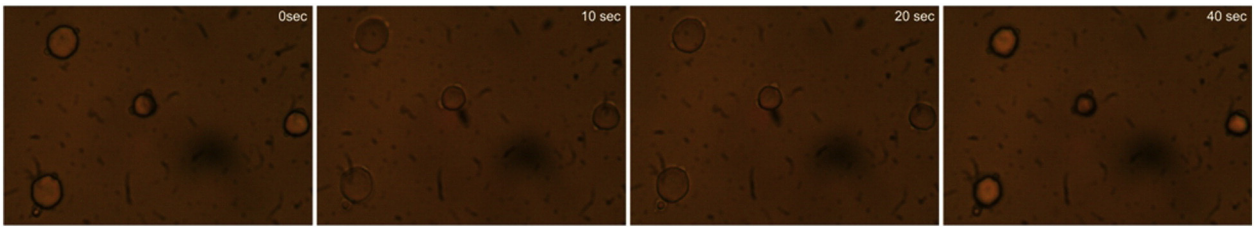

Fig. 3. The phase-contrast image of erythrocyte ghosts, in the course of VL low concentration venom-treatment. Erythrocyte ghosts were prepared as described in Section 2.4. Dried lyophilized toxin of VL was dissolved in Tris-HCl buffer (pH 7.4) with a final concentration of $3 * 10^{-5}$ M, and 1.1 μL of this solution were added to the microscope sample.

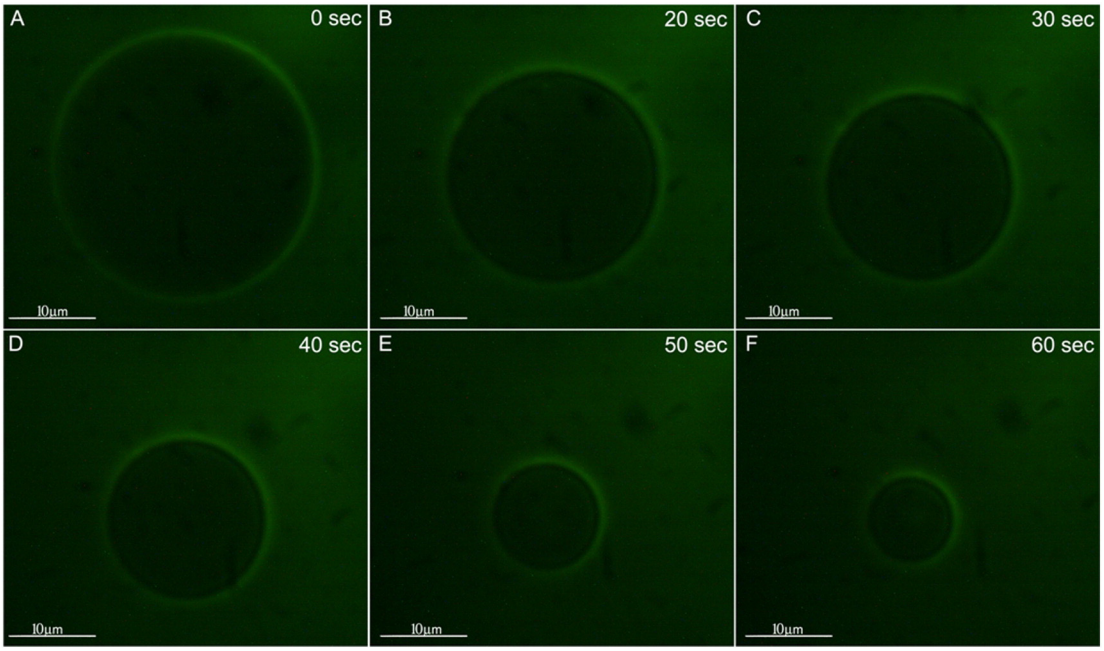

Fig. 4. Time-dependent decreasing of the ANS-containing erythrocyte ghosts, in the course of VL venom processing (60 s). ANS labeling was done as described in Section 2.5. Dried lyophilized toxin of VL was dissolved in Tris-HCl buffer (pH 7.4) with a final concentration of $3 * 10^{-5}$ M, and 1.1 μL of this solution were added to the microscope sample.

lost the initial membrane lipid/protein ratio and sugar asymmetry responsible for the high optical contrast seen in the first snapshot. The last snapshot (40 s) shows the treated condition of the RBCs, which are clearly smaller than the original vesicles and shows a rethickening of the membrane (Fig. 3D).

For fluorescent microscopy the membrane fluorescence probe ANS (8-anilino-1-naphthalene sulfonic acid) was used to visualize erythrocyte ghosts. ANS integrates into the membrane and emits with sufficient intensity to follow the changes produced on the RBCs after the addition of the venom. One selected representative sequence is shown in Fig. 4: erythrocyte ghost show a homogeneous distribution of the fluorescent probe used, ANS, attesting that the lipid content of the erythrocyte membrane did not exhibit detectable phase separation (see snapshots at 0 and 60 s in Fig. 4). The main effect caused by VL venom was the dramatically decrease of erythrocyte size without any detectable changes of shape and fluorescence intensity.

3.2. Visualization of GUV morphological changes by fluorescence measurements

The phospholipid extract were used to form GUVs, which retained the complexity in lipid composition of the original cells adequately

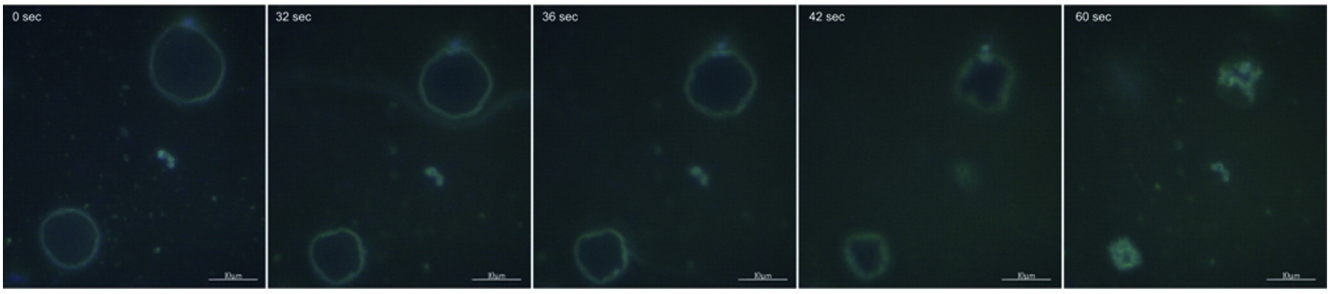

Fig. 5. Rapid changes of the fluorescent intensity of the ANS-containing GUVs in the course of VL venom processing (60 s). ANS labeling was done as described in Section 2.5. GUVs were prepared according to the electroformation method in a temperature-controlled chamber containing Tris-HCl buffer (pH 7.4). Dried lyophilized toxin of VL was dissolved in the same buffer (Tris–HCl, pH 7.4) with a final concentration of $3 * 10^{-5}$ M, and 2.2 μL of this solution was added to the fluorescent microscope sample.

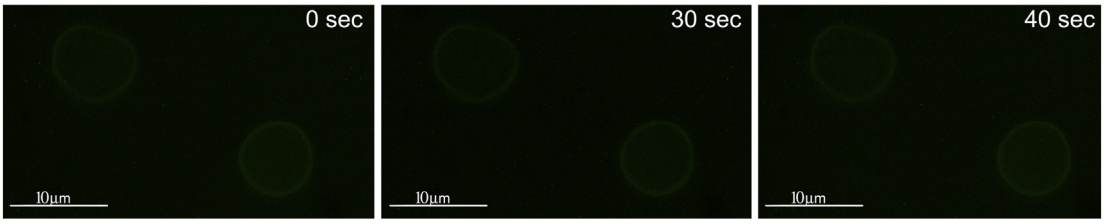

Fig. 6. The fluorescent image of GUVs after *Vipera latifi* low concentration venom-treatment. GUVs were tried to prepare according to the electroformation method in a temperature-controlled chamber containing Tris-HCl buffer (pH 7.4). Dried lyophilized toxin of VL was dissolved in Tris-HCl buffer (pH 7.4) with a final concentration of $3 * 10^{-5}$ M, and 1.1 μL of this solution were added to the fluorescent microscope sample.

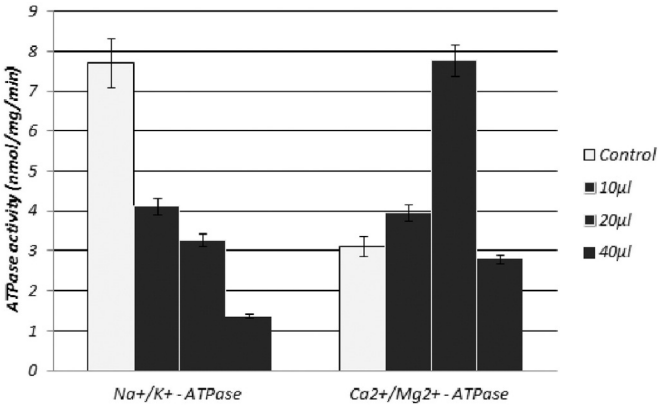

Fig. 7. Na^+/K^+ and Ca^{2+}/Mg^{2+}-ATPase activity in *Vipera latifi* venom-treated erythrocyte ghosts. Enzymatic activity was assayed as described in Section 2.6 for three concentrations of snake venom and expressed nmol Pi released/mg protein/min. The columns are the mean ± S.D. (n = 6). $P < 0.05$ *vs.* the control group (ANOVA followed by the Bonferroni test).

mimicking the erythrocyte ghost's size and curvature. On the other hand, we have a quite simple and commonly used biomimetic system free of its protein components. GUVs also were visualized with the membrane fluorophore ANS during experiments on VL venom hydrolysis. Fig. 5 shows the drastic decreasing of liposomes in course of modification with a lethal concentration of venom at 21 °C in the liquid phase. The insertion of venom leads to the very fast shrinking and corrugation of GUVs membrane, after which the vesicle shrinks until nothing (last snapshot). But intriguingly the lower concentrations of venom (sub-lethal) didn't cause any changes at all (Fig. 6).

3.3. Na^+/K^+ and Ca^{2+}/Mg^{2+}-ATPase activity in venom-treated erythrocyte ghosts

The other series of experiments was done with a determination of RBC membrane's main ion transporters activities in course of treatment with *Vipera latifi* venom. The *in vitro* treatment of erythrocyte ghosts with VL venom significally inhibit the Na^+/K^+-ATPase activity (Fig. 7), which were accompanied by a significant increase in RBC Ca^{2+}/Mg^{2+}-ATPase activity 10 min after addition of the low concentration of venom, compared to control erythrocyte ghosts (Fig. 7). The treatment with gradually increasing concentrations of venom revealed the dose dependent manner of Na^+/K^+-ATPases activity inhibition for so called sub-lethal and lethal concentrations (pharmacologically relevant to the half of LD50 dose and LD50 dose, respectively). For these concentration of venom the activity of Ca^{2+}/Mg^{2+}-ATPase, on the contrary, increasing very dramatically compare with the control data. For higher concentration it was impossible to obtain a countable data because of the fatal damage of membrane lead to the complete lysis of erythrocyte ghosts.

4. Conclusions and perspectives

The snakebites with viper venom produced extensive systemic alterations, including tissue blistering, oedema, hemorrhage and necrosis, as well as hypotension shock and coagulopathy, especially clotting disorders and hypofibrinogenemia (Kakanj et al., 2015; Sanz et al., 2008; Ayvazyan and Ghazaryan, 2012). The damage concern primarily blood cells and the resistance of erythrocytes to the envenomation in this respect became quite crucial issue.

Vipera latifi is a very endemic species in Iran and any investigations of its toxinology and envenomation effects are very scarce, but the distribution of these snakes in the country is quite wide, so the studying of these snake venoms either by itself or in comparison with other viper venoms of the region become more and more important. Our previous research was devoted to the molecular events associated with *Macrovipera lebetina obtusa* and *Montivipera raddei* snakes' venom intoxication and condition of biomembranes (Ayvazyan and Ghazaryan, 2012; Ayvazyan et al., 2012). These two species of snakes together with *Vipera latifi* are the most pharmacologically important *Viperidae* snakes of Iran and detailed analysis of their membranotropic properties quite vital both for antivenom production in the country and opening of new perspectives in drug design and development.

The present study confirmed the direct damage of red blood cell membranes by VL venom components, and the fast transformation of erythrocytes in course of envenomation. It also showed that morphological changes of red blood cells caused by venom injection could be reversible depend on the venom concentration in media. The study underlines that drastic changes during venom treatment occur both in the lipid composition of membranes and the main protein systems within the membranes, like ATPase complexes. These functional alterations could be also caused by the changes in lipid bilayer packaging in the RBCs membrane, its plastic properties, fluidity and microviscosity. The inhibition of Na^+/K^+ and Ca^{2+}/Mg^{2+}-ATPase activities in venom-treated erythrocyte ghosts conclusively shows that viper venom has a profound restructuring effect on the lateral organization of lipids in model and complex biological membranes. Moreover, our data for higher concentration of venom let us suggest, that venom components mainly blocking the work of Na^+/K^+ pump. Together with the damage of lipid packaging these changes cause the drastic increasing of Ca^{2+} cations in the erythrocytes and leading to the activation of Ca^{2+}/Mg^{2+}-ATPase work. The present observations on the Ca^{2+} pump ATPase activity in RBCs of subjects with intoxication may be taken to suggest that the activity of this membrane-associated pump is not altered irreversible. The Ca^{2+} pump ATPase is the only mechanism by which RBCs maintain low intracellular Ca^{2+} concentration and an important means by which other cells accomplish this. Maintenance of low intracellular Ca^{2+} concentration is critical for normal cell function and viability. It is known, that even 20% decrease in activity of the Ca^{2+} pump ATPase in the RBCs (for example, of hypertensive subjects) may reflect a deficit in the ability of certain cells to maintain optimally low intracellular Ca^{2+} (Farber, 1981). Current observation of the enhanced activity of Ca^{2+}/Mg^{2+}-ATPase could be an attempt to indirectly counteract the Ca^{2+} overload, *i.e.* Ca^{2+} extrusion through the Na^+/Ca^{2+} exchanger operating in forward mode. Based on these considerations, we suggest that the enhanced activity of Ca^{2+} pump ATPase seen after treatment with VL venom may be a protective mechanism aimed at preserving erythrocyte ghosts' cytoskeletal function during membrane damage. This conclusion agrees with our previous observation, that erythrocyte membrane damage could be reversible for low concentrations of venom, but irreversible for the increased dose of toxins. As a conclusion of present experimental observation, we think that VL venom components damaging the lipid bilayer of erythrocyte membrane, which cause the multiple defects in the bilayer packaging and, hence the outwardly directed efflux of K^+ ions from erythrocyte and increase inward of Ca^{2+} ions gradient. It seems to us logical to suggest that Ca^{2+}/Mg^{2+}-ATPase is not significantly damaged by the venom components, but because of this dramatic changes of cation exchange through RBC membrane, the activity of Ca^{2+} pump ATPase used to increase almost twice compare to the normal conditions. Clearly, as well as its numerous benefits, there are limitations to studying mechanisms of action of molecules on erythrocyte ghosts and GUVs, as there are with any model systems. But such a complex experiments of erythrocyte ghosts in comparison with lipid vesicles as a negative control without protein components, seems to us very perspective for future investigations.

Conflict of interests

The authors declare no conflict of interests.

Acknowledgements

This work was supported by Grant # 3575-CE from the Armenian National Science and Education Fund (ANSEF) based in New York, USA.

References

Angelova, M., Soleau, S., et al., 1992. Preparation of giant vesicles by external fields. Kinetics and application. Progr. Colloid Polym. Sci. 89, 127–131.

Ayvazyan, N.M., Ghazaryan, N.A., 2012. Lipid bilayer condition abnormalities following *Macrovipera lebetina obtusa* snake envenomation. Toxicon 60 (4), 607–613.

Ayvazyan, N.M., Zaqarian, N.A., Ghazaryan, N.A., 2012. Molecular events associated with *Macrovipera lebetina obtusa* and *Montivipera raddei* venom intoxication and condition of biomembranes. Biochim. Biophys. Acta Biomembr. 1818 (5), 1359–1364.

Babu, N., 2009. Influence of hypercholesterolemia on deformability and shape parameters of erythrocytes in hyperglycemic subjects. Clin. Hemorheol. Microcirc. 41 (3), 169–177.

Coka-Guevara, S., Markus, R.P., Caruso-Neves, C., Lopes, A.G., Vieyra, A., 1999. Adenosine inhibits the renal plasma-membrane (Ca^{2+} + Mg^{2+})-ATPase through a pathway sensitive to cholera toxin and sphingosine. Eur. J. Biochem. 263, 71–78.

Dehghani, R., Fathi, B., Panjeh Shah, M., Jazayeri, M., 2014. Ten years of snakebites in Iran. Toxicon 90, 291–298.

Dodge, J.T., Mitchell, C., Hanahan, D.J., 1956. Arch. Biochem. Biophys. Acta 100, 119–230.

Elgsaeter, A., Mikkelsen, A., 1991. Shapes and shape changes in vitro in normal red blood cells. Biochim. Biophys. Acta 1071, 273–290.

Elgsaeter, A., Stokke, B.T., Mikkelsen, A., Branton, D., 1986. The molecular basis of erythrocyte shape. Science 234, 1217–1223.

Farber, J.L., 1981. The role of calcium in cell death. Life Sci. 29, 1289–1295.

Fiske, C.H., Subbarrow, Y., 1925. The colorimetric determination of phosphorous. J. Biol. Chem. 66, 375–400.

Flachsenberger, W., Leigh, C.M., Mirtschin, P.J., 1995. Sphero-echinocytosis of human red blood cells caused by snake, red-back spider, bee and blue-ringed octopus venoms and its inhibition by snake sera. Toxicon 33, 791–797.

Ghazaryan, N.A., Ghulikyan, L., Kishmiryan, A., Kirakosyan, G., Nazaryan, O., Ghevondyan, T., Zakaryan, N., Ayvazyan, N., 2015a. Anti-tumor effect investigation of obtustatin and crude *Macrovipera lebetina obtusa* venom in S-180 sarcoma bearing mice. Eur. J. Pharmacol. 764, 340–345.

Ghazaryan, N.A., Ghulikyan, L., Kishmiryan, A., Andreeva, T.V., Utkin Yu, N., Tsetlin, V.I., Lomonte, B., Ayvazyan, N.M., 2015b. Phospholipases A_2 from *Viperidae* snakes: differences in membranotropic activity between enzymatically active toxin and its inactive isoforms. Biochim. Biophys. Acta Biomembr. 1848 (2), 463–468.

Hesketh, J.E., London, J.B., Reading, H.W., Glen, A.I., 1978. The effect of lithium treatment on erythrocyte membrane ATPase activities and erythrocyte ion content. Br. J. Clin. Pharmacol. 5, 323–329.

Ibrahim, S.A., Thompson, R.H., 1965. Action of phospholipase a on human red cell ghosts and intact erythrocytes. Biochim. Biophys. Acta 99, 331–341.

Kakanj, M., Ghazi-Khansari, M., Mirakabadi, A.Z., Daraei, B., Vatanpour, H., 2015. Cytotoxic 326 Effect of Iranian Vipera lebetina Snake Venom on HUVEC Cells. Iranian Journal of 327 Pharmaceutical Research 14 (Supplement), 109–114.

Kassák, P., Sikurová, L., Kvasnicka, P., Bryszewska, M., 2006. The response of Na+/K+-ATPase of human erythrocytes to green laser light treatment. Physiol. Res. 55 (2), 189–194.

Klop, B., van de Geijn, G.-J.M., Bovenberg, S.A., van der Meulen, N., Elte, J.W.F., et al., 2013. Erythrocyte-bound apolipoprotein B in relation to atherosclerosis, serum lipids and ABO blood group. PLoS One 8 (9), e75573.

Latifi, M., 1984. Variation in yield and lethality of venoms from Iranian snakes. Toxicon 22 (3), 373–380.

Latifi, M., 1991. The Snakes of Iran. Society for the Study of Amphibians and Reptiles, Oxford, Ohio, USA.

Latifi, M., Shamloo, K., Amin, A., 1965. Characteristic electrophoretic patterns of serum proteins of several species of snakes of Iran. Can. J. Biochem. 43, 459–461.

Lenk, P., Kalyabina, S., Wink, M., Joger, U., 2001. Evolutionary relationships among the true vipers (Reptilia: Viperidae) inferred from mitochondrial DNA sequences. Mol. Phylogenet. Evol. 19, 94–104.

Lowry, O.H., Rosebroughr, N.J., Farr, A.L., Randall, R.J., 1951. J. Biol. Chem. 193, 265–275.

Mueller, P., Rudin, D., Tien, H., Wescot, T., 1962. Reconstruction of cell membranes structure in vitro and its transformation into an excitable system. Nature 194, 979–980.

Nilson, G., Tuniyev, B., Andrén, C., Orlov, N., Joger, U., Herrmann, H.W., 1999. Taxonomic position of the *Vipera xanthina* complex. Kaupia 8, 99–102.

Oliveira, S., Saldanha, C., 2010. An overview about erythrocyte membrane. Clin. Hemorheol. Microcirc. 44, 63–74.

Pasini, E.M., Kirkegaard, M., Mortensen, P., Lutz, H.U., Thomas, A., Mann, M., 2006. In-depth analysis of the membrane and cytosolic proteome of red blood cells. Blood 108, 791–801.

Sanchez, S., Chen, et al., 2001. Solution and interface aggregation states of *Crotalus atrox* venom phospholipase A_2 by two-photon excitation fluorescence correlation spectroscopy. Biochemistry 40, 6903–6911.

Sanz, L., Ayvazyan, N., Calvete, J.J., 2008. Snake venomics of the Armenian mountain vipers *Macrovipera lebetina obtusa* and *Vipera raddei*. J. Proteome 71 (2), 198–209.

Verstraeten, S., Hammerstone, J., et al., 2005. Antioxidant and membrane effects of procyanidin dimmers and trimers isolated from peanut and cocoa. J. Agric. Food Chem. 53, 5041–5048.

Vincenzi, F.F., Morris, C.D., Kinsel, L.B., Kenny, M., McCarron, D.A., 1986. Decreased calcium pump adenosine triphosphatase in red blood cells of hypertensive subjects. Hypertension 8, 1058–1066.

Wallach, V., Williams, K.L., Boundy, J., 2014. Snakes of the World: a Catalogue of Living and Extinct Species. CRC Press, Boca Raton.

Yau, T.W., Kuchel, R.P., Koh, J.M.S., Szekely, D., Mirtschin, P.J., Kuchel, P.W., 2012. Cytoskeletal rearrangements in human red blood cells induced by snake venoms: light microscopy of shapes and NMR studies of membrane function. Cell Biol. Int. 36, 87–97.